Sudan University of Science and Technology

College of Engineering

Biomedical Engineering Department

Accuracy Analysis For Anatomical Landmarks Based Registration in Image Guided Neurosurgery

تحليل دقة استخدام التسجيل بواسطة المعالم التشريحية في الجراحة العصبية الموجهة بالصور

A research submitted in partial fulfillment for the requirements of the degree of B.Sc. (Honors) in Biomedical Engineering

Prepared By:

1. ADEN HASSAN MARGANI EL.SANOUSI
2. FATIMA ABDALLA ALTYEB MUSTAFA
3. METHA IBRAHIEM BASHER YAHIA

Supervised By:

Dr. AKRAM ISMAIL

October 2015

الأيـة

قال تعالى:

﴿ الله نور السموات والأرض مثل نوره كمشكوة
فيها مصباح المصباح في زجاجة الزجاجة كأنها
كوكب دري يوقد من شجرة مباركة زيتونة لا
شرقية ولا غربية يكاد زيتها يضئ ولو لم تمسسه نار
نور على نور يهدي الله بنوره من يشاء ويضرب الله
الأمثال للناس والله بكل شئ عليم ﴾

سورة النور- الأية(35)

DEDICATION

We dedicate our success to the failures we faced, the obstacles we overcomed and to the people who were there supporting us, raising our spirits high whenever accomplishment seems impossible. Thanks to their presence in our lives we had no fear of failure; we knew for sure that whenever we hit the bottom their loving hearts will lift us up.

To you ***mother*** *for holding my hand since my day one in life. Without your tender, guiding and sometimes over protecting touch I would have never became who I am today, I am your creation.*

To my mountain, who taught me to stand high, to feel proud of whom I am and not to fear falling rocks because I am stronger. To you ***father****.*

To you my ***friends,*** *who know me, but love me anyway. Without you I can never make do in this world.*

Acknowledgements

First and foremost, We would like to thank ***Allah*** *for giving our the strength and guidance to accomplish our thesis. Without His guidance, we will certainly not be able to complete this task successfully.*

To our generous supervisors, and Dr. ***Akram Ismail Mohammed,*** *thank you for your generous support and intellectual guidance throughout our year as graduate students.*

To our ***parents*** *who had given us all the supports that we need not only to complete this project but also from the beginning of our life in the university.*

Finally, our thanks to all the staff of Bio-Medical Engineering Department.

Table of figures

Table of Tables:

Abbreviations

IGS	Image Guided Surgery
IGNS	Image Guided Neurosurgery
SM/ASM	Skin Markers/Adhesive Skin Maker
NM	Natural Markers
CT	Computed Tomography
MRI	Magnetic Resonance Imaging
IV	Integral Videography
PET	Positron Emission Tomography
OR	Operating Room
FM	Fiducial marker
BMM	Bone-Mounted Markers
ALS	Anatomical Landmark
FLE	Fiducial Localization Error
TRE	Target Registration Error
FRE	*Fiducial Registration Error*
RMS	Root Mean Square

ABSTRACT

Application of image guided surgery methods provide less invasive surgery, its accuracy depend upon registration methods Accurate patient to image registration is the core for successful and safe image-guided neurosurgery. Point-matching is the most common technique in practice to achieve this registration.

This project is developed using MATLAB to analyze the accuracy of anatomical landmarks to be used as Fiducial points for point based registration method in image guided neurosurgery thus to avoid the problems of the other marker used for the same purpose. Three kinds of results are calculated in this project and they were**:** Subjectivity Analysis Result with fiducial registration error (FRE) value equal to 2.3816 ± 1.4955 for thirty random samples. Repetitive Selection result with standard deviation from fiducial registration error (FRE) value equal to 0.6053. finally the comparison of target registration error variation within the head.

المستخلص

ان تطبيق طرق الجراحة الموجهة بالصور توفر أقل تدخل جراحي وتعتمد دقتها على طرق التسجيل,ان التسجيل الدقيق بين المريض والصور هو صميم الجراحة العصبية الناجحة والامنة . مماثلة النقاط هي الاسلوب الاكثر تطبيقا لتحقيق هذا التسجيل.

هذا المشروع تم تطويره باستخدام الماتلاب لتحليل دقة استخدام المعالم التشريحية كنقاط موثوثة لعملية التسجيل المستخدمة في الجراحة العصبية الموجهة بالصور لتفادي مشاكل المعالم الاخرى المستخدمة لنفس الغرض . في هذا المشروع تم حساب ثلاثة انواع من النتائج وهي :نتيجة اختلاف الاشخاص في اختيار نفس النقطة وقيمة خطأ التسجيل الموثوق المحسوبة لها تساوي 2.3816 ± 1.4955 لثلاثين عينة عشوائية .نتيجة الاختيار المتتالي لنفس النقطة بانحراف معياري عن قيمة خطأ التسجيل الموثوق المحسوبة يساوي 0.6053 , اخيرا مقارنة الفيم المختلفة لخطا التسحيل للهدف في الراس.

CHAPTER ONE

INTRODUCTION

1.1 General view

Surgeons have traditionally performed procedures to treat diseases by gaining direct access to the internal structures involved, and using direct visual inspection to diagnose and treat the defects. Much effort has gone into identifying the most appropriate incisions and approaches to enable full access inside body cavities, specific organs, or musculoskeletal structures. [1]

Image guided surgical methods are providing a surgeon with the ability to visualize internal structures and their geometric relationships, we have relied on a registration method that finds the best alignment between image volume and physical volume, based on the alignment of all the data in the volumes.[2]

1.2 Problem statement

Neurosurgeons require high accuracy, less invasiveness technique to perform surgeries .technique used is actually depend on registration.

Ascertain accuracy of anatomical landmark to be used as registrations points allow us to use it instead of the other marker's kind thus avoid their problems.

1.3 Objective

Assess the applicability and accuracy of anatomical landmark for registration in image guided neurosurgery to establish the relationship between the location of surgical instruments used by neurosurgeon and patient's anatomy.

1.4 Methodology

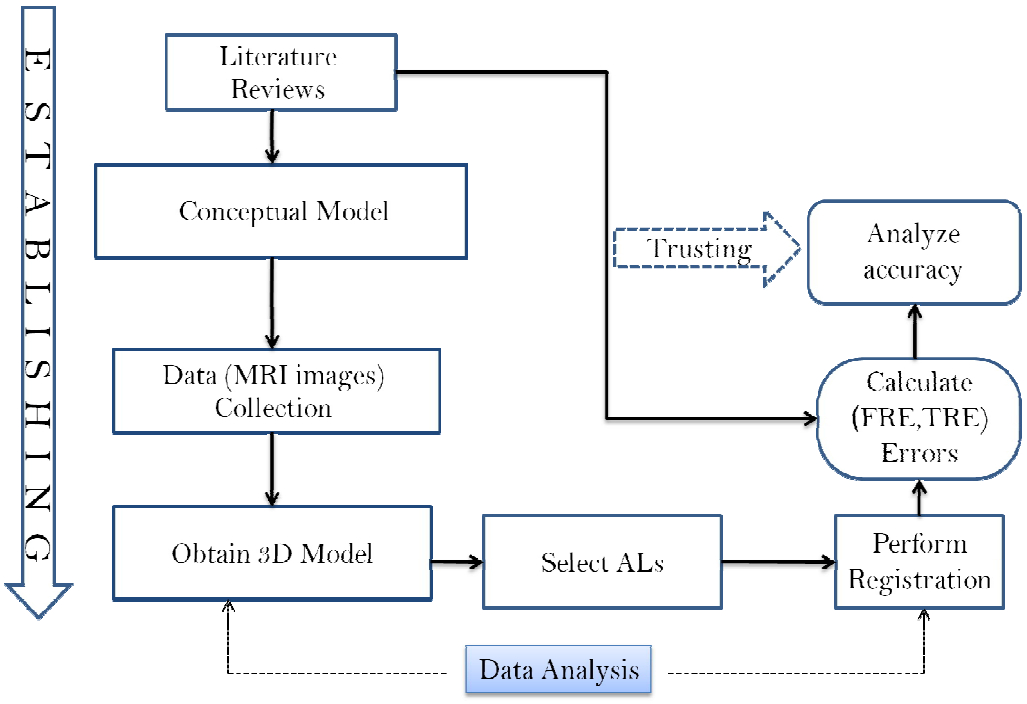

Figure 1.1 Methodology

Following the above figure _ explained in detail in chapter four_

Steps mentioned below were followed

i. Prepare registration data.
ii. Perform registration based anatomical landmark.
iii. Analyze the accuracy.

1.5 Motivations

Image guided surgery (IGS) requires a registration between an object in physical space and the same object in image space. Registration is either point-pair matching or surface matching. The most common method used is point based registration. The most effective point based registration uses extrinsic objects that are attached to patients. These extrinsic objects and anatomic landmarks are referred to as fiducial markers.

Extrinsic objects may be anatomical land mark or skin adhesive marker. Anatomical landmarks are well-defined points in the anatomy that experts use to establish biologically meaningful correspondences between structures.

Using of skin marker is partly limited by the preoperative planning procedures, which include application of (SM) and planning radiography for intraoperative patient-to-image registration. The application of the commonly used self-adhesive SM is time-consuming,

Requires trained personnel, and causes patient discomfort, as shaving may be necessary. Once applied, the SM tends to move or even fall off with time, so that the registration accuracy is inversely related to the duration between planning procedures and registration. The planning radiography is again time-consuming and, in the case of CT, causes additional effects of radiation on the patient. Magnetic resonance

imaging can be difficult to obtain in time and – as diagnostic images are already available in every patient – may be a redundant additional imaging procedure.

The application of anatomic landmarks as (NM) instead of SM may overcome the problem of preoperative patient discomfort and could save staff and imaging time by use of the diagnostic MRI for intraoperative registration. Therefore, we conducted a prospective study to evaluate whether the use of NM is both applicable and accurate [3]

1.6 Project Layout

The research include six chapters, **Chapter one** consist of introduction, literature was reviews in **Chapter two ,**theoretical background described in **Chapter three**, methodology explained in **Chapter four,** results and discussion of the research is described in **Chapter five**, **Chapter six** included conclusions and recommendations.

CAHPTER TWO

LITRATURE REVIEWS

“Stefan Wolfsberger · K. Rössler · R. RegatschnigK. Ungersböck published “

The study conducted to evaluate whether the use of NM compared to conventional SM is both applicable and accurate. The accuracy of NM was evaluated in 26 patients operated on in the supine (*n*=24) or sitting (*n*=2) position. In 21 cases, NM were compared to SM with planning radiography.

The root mean square error (RMSE) of the registered volume was Calculated by the Philips Easy Guide Neuro frameless stereotactic navigation system and compared between the two registrations modalities. The mean RMSE was 3.2 mm±1.0 mm standard deviation using NM vs. 2.9±1.0 mm using skin-adhesive SM (*P*=0.13, Student’s *t*-test). Computed tomography was slightly more accurate than MRI planning (mean RMSE 3.2 mm vs. 3.3 mm). In three cases, diagnostic radiography (MRI) was used with a mean RMSE of 5.3 mm but acceptable intraoperative landmark correlation. [3]

“ Erasmo Barros da Silva Jr. & André G. Leal & Jerônimo B. Milano & Luis F. Moura da Silva Jr. & Rogério S. Clemente & Ricardo Ramina introduced “

The goal was to determine the accuracy of this navigation technique and to establish the relationship between the location of the asterion and the transverse and sigmoid sinuses junction TSSJ.

Magnetic resonance imaging (MRI) T1 sequences with gadolinium (FSPGR with FatSst, 1.5 T GE® Signa) and frameless navigation (Vector vision®, Brainlab®) were used for surgical planning. Registration was performed using six anatomical landmarks.

Results show that navigation enabled the location of the TSSJ and the emissary vein, with an accuracy flaw below 2 mm. [4]

"Wolfgang K. Pfisterer, M.D., Wolfgang K. Pfisterer, M.D. and Denise A. Drumm, Ph.D published".

The goal was to determine the concordance among a point-merged FM registration, a point-merged AL registration, and a combined point-merged anatomic/surface-merged registration, i.e., to determine the accuracy of registration techniques with and without FMs by examining the extent of agreement between the system-generated predicted value and physical measured values.

30 volunteers were examined and treated with gamma knife surgery. The frameless stereotactic image-guidance system called the Stealth Station (Medtronic Surgical Navigation Technologies, Louisville, CO) was used. Nine FMs were placed on the patient's head and four were placed on a Leksell frame rod-box, which acted as a rigid set to determine the difference in error. For each registration form, generated measurement (GM) and the physical measurement (PM) to each of the four checkpoint FMs was recorded. The mean of values for GMs were 1.14 mm for FM, 2.3 mm for AL, and 0.96 mm for SM registrations. The mean errors of the checkpoints were 3.49 mm for FM, 3.96 mm for AL, and 3.33 mm for SM registrations. [5]

"M. Ovinis, D. Kerr, K. Bouazza-Marouf, and M. Vloeberghs published "

In this study algorithms for the automatic localisation of canthus (inner corner of the eye) and tragus (a small, pointed, cartilaginous flap of the ear), were described in CT images. The approach was tested on a dataset of near isotropic CT images of 95 patients. The position of the automatically localised landmarks was compared to the position of

The manually localised landmarks. The average difference was.1mm and 0.8 mm for the medial canthus and tragus, with a maximum Difference of 4.5 mm and 2.6 mm respectively The medial canthus and tragus can be automatically localized in ct images with performance comparable to manual localization. [6]

CAHPTER THREE

THEORETICAL BACKGROUND

3.1 Surface Anatomy of the Head

The human head consists of a fleshy outer portion surrounded by the bony skull, within which sits the brain. [7] The head rests on the neck, and is provided bony support for movement by the seven cervical vertebrae.

3.1.1 The skull

It is made up mainly of two main parts

Cranium

The soft parts covering the upper surface of the skull form the scalp and include the frontal, occipital, sphenoid, ethmoid and two paired bones: the parietal and temporal.[8] (Figure 3.1)

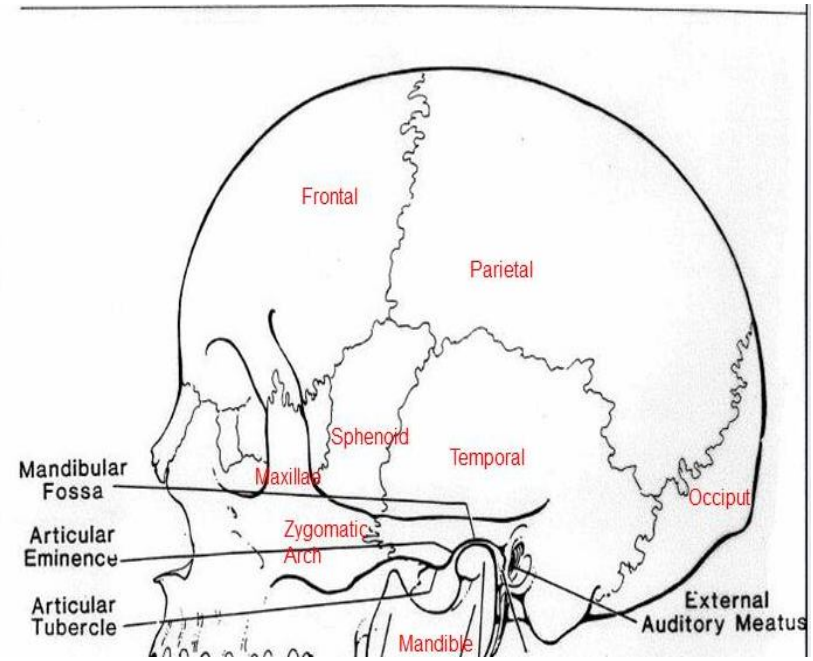

Figure 3.1 view of the skull region [8]

Facial bones

The facial bones consist of 14 bones that make up the lower front of the skull. Facial bones along with the frontal bone of the cranium, which constitutes the top of the face above eyeballs, are the most important bones for the appearance of the face. [9]

3.1.2 Brain

The general outline of the cerebral hemisphere on either side may be mapped out on the surface in the following manner. Starting from the nasion a line drawn along the middle of the scalp to the inion represents the superior border. The line of the lower margin behind is that of the transverse sinus or more roughly a line convex upward from the inion to the posterior root of the zygomatic process of the temporal bone; thence

along the posterior two-thirds of the upper border of the zygomatic arch where the line turns up to the pterion; the front part of the lower margin extends from the pterion to the glabella about 1 cm. above the supraorbital margin [8].

3.1.3 Anatomical Landmarks of the Head

They are distinct reference points in the surface of the face and head. These landmarks are visual surface representation of slightly deeper structures such as bones, cartilages, muscles and tendons. They are usually defined at protuberances tips, joint junctions, lines ends and sutures intersections. [9]

3.1.4 Bony Landmarks

The bony points already described which can be determined by palpation, the following are utilized for surface markings.

Auricular Point

The center of the orifice of the external acoustic meatus.

Preauricular Point

A point on the posterior root of the zygomatic arch immediately in front of the external acoustic meatus.

Asterion.

oparietalmast sutures The point of meeting of the lambdoidal, mastoöccipital,

Pterion

The point where the great wing of the sphenoid joins the sphenoidal angle of the parietal .

Inion

The external occipital protuberance.

Lambda

The point of meeting of the lambdoidal and sagittal sutures

Bregma

The meeting-point of the coronal and sagittal sutures; it lies at the point of intersection of the middle line of the scalp with a line drawn vertically upward through the preauricular point.

Reid's base line

A line passing through the inferior margin of the orbit and the auricular point

lambdoidal suture

Can be indicated on either side by the upper two-thirds of a line from the lambda to the tip of the mastoid process.

sagittal suture

Is in the line joining the lambda to the bregma.[8]

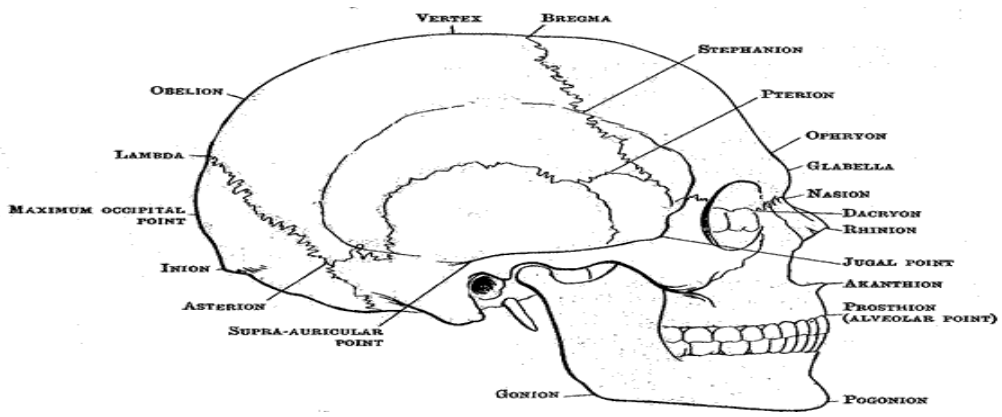

. Figure 3.2 view for some of the skull's landmarks [9].

3.2 Image Guided Surgery

Recent developments in computer vision and robotics are changing the manner in which modern surgery is being practiced. Motivated by better results and lower overall costs, clinical practice is rapidly replacing traditional open surgical procedures with minimally invasive techniques. Most notably this is a transition from direct visual feedback to indirect, image-based feedback.

This transition is not without its challenges. In open surgery the physician can directly see and feel the anatomical structures. In image-guided procedures, the physician needs to identify anatomical structures in the images (segmentation), and mentally establish the spatial relationship between the imagery and the patient (registration). Additionally, the procedure's execution accuracy should be comparable or better than that achieved by the traditional approach (navigation).These requirements create a steep learning curve, and increase the dependency of a favorable outcome on the physician's ability to mentally recreate the spatial situation and transfer a plan into action

Image-guided systems aim at augmenting and complementing the physician's ability to understand the spatial structure of the anatomy by

integrating medical images and other sources of information [10], such as tracked instruments. These systems potentially have a three-fold effect:

1. They can mitigate the learning curve for minimally invasive procedures and reduce the variability of the outcome, narrowing the gap between exceptional and standard practice.
2. They may enable new minimally invasive procedures, allowing physicians to perform procedures that were previously considered too dangerous.
3. they transform qualitative procedure evaluations into quantitative ones, enabling a quantitative comparison between plan and execution.

Image-guidance systems were initially accepted by two medical disciplines; neurosurgery and orthopedics .The main reason for this early adoption is that both disciplines accommodate the use of a rigid anatomy assumption. In neurosurgery the brain's motion is constrained by the skull, although brain shift is an issue and has been the subject of much research. In orthopedics the assumption is always valid.

Current commercial image-guided systems are all based on a rigid anatomy assumption. Image-guided systems for deformable anatomical structures are still a subject of research.

3.2.1 Configuration of the image guided system

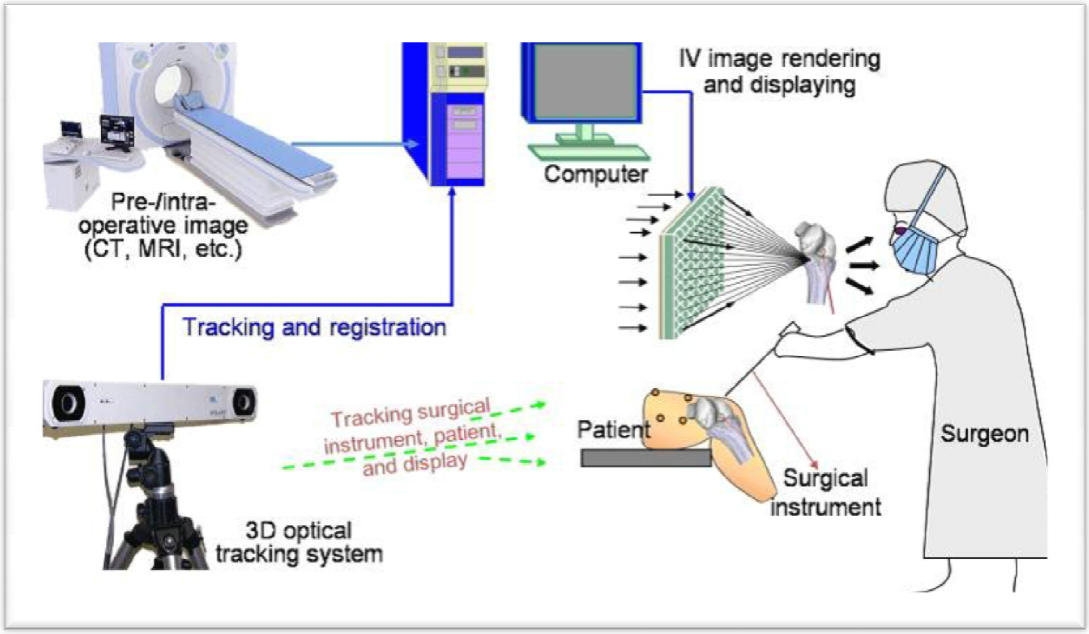

Figure 3.3 System configurations [11]

Image acquisition device (pre_/intra-operative imaging)

The main sources of information for image-guided procedures are the medical images themselves.

Table 3.1 Classification of imaging devices according to their availability for intra-operative use, their accessibility to physicians around the world, the dimensionality of the data they acquire and the type of information conveyed by the images

Modality	Intra-operative Availability	Accessibility	Data Dimensionality
Computed Tomography (CT)	available (not widespread)	High	3D
Magnetic Resonance Imaging (MRI)	available (not widespread)	High	3D

X-ray	Available	High	2D projection
functional Magnetic Resonance Imaging (fMRI)	not available	Moderate	3D
Positron Emission Tomography (PET)	not available	Moderate	3D
Single Photon Emission Computed Tomography (SPECT)	not available	Moderate	3D
X-ray Fluoroscopy	Available	High	2D projection
C-arm CT	Available	Low	3D
Ultrasound (US)	Available	High	2D
optical imaging	Available	High	2D projection

Instrument Tracking

Applications of instrument tracking include automatic instrument control and improved image displays. Instrument tracking consists of determining the relationship between the instrument, the anatomy, and the image coordinate frame. Two methods exist for automatically determining this relationship:

External and Image-based tracking. External methods make use of standalone measurement equipment for localization; whereas image based methods require image analysis.

integral videography (IV)image rendering and display

During the operation, images are displayed on normal and IV Displays IV records and reproduces 3-D images by using a micro convex lens array and a high-pixel-density flat display, e.g., an LCD display.

3.2.2 Image guided system phases

Image-guided procedures are described using a time-line based view. The three phases of a procedure are: pre operative planning, intra-operative plan execution, and post-operative assessment. This is an idealized view, but it is useful in that it encompasses all the steps of an image-guided procedure. [9]

Pre-operative planning

In this phase the goal is to create a surgical plan based on pre-operative images and additional information such as implant geometry or functional information. Multiple imaging modalities may be used concurrently, such as CT and MRI for optimal bone and soft tissue visualization, or CT and PET to correlate functional and anatomical data. Plans are formulated in a single coordinate system to which all data is mapped. These plans are patient and procedure specific and have variable complexity. The complexity can range from simple plans such as specifying a target and trajectory for a biopsy, to moderately complex plans such as choosing and positioning implants, to complex plans incorporating physically based simulations of joint movements and interactions between soft tissue and bone structures.

Intra-operative plan execution

Once the patient is in the operating room (OR), the coordinate system in which the plan was specified must be aligned to a coordinate system in the

OR. The image-guided system now provides visual assistance to the physician, by tracking tools and anatomical structures and displaying their spatial relationships, using a variety of interfaces and displays. Additional information, such as intra-operative images, may be acquired to update the anatomical picture. If necessary, the procedure plan is then modified. During the procedure the guidance system can record the spatial relationships between the tools and the anatomy. This data can later be used for quantitative assessment of the intervention and for training purposes.

Post-operative assessment

Post-operative images are acquired and the results of the procedure are quantitatively compared to the pre-operative plan.

3 .2.3 image guided system application

The image guided systems started, developed and matured in the field of neurosurgery, adapted to it is applications. One of their first practices outside the brain is their use in spinal surgeries which stemmed from the fact that both fields shared the benefit of the available rigid anatomy. In addition, both fields require accurate guidance to ensure less harm to their content of functionally important tissues. The rigid body assumption is not hundred percent true in both cases due to the phenomena of soft tissue motion inside the skull known as brain shift and due to the spinal cord motion. While spinal cord vertebras are actually rigid if considered individually, but as whole cord still can exhibit changes in length, movements and shifts due to the presence of the deformable disks between the vertebras.

Even thought spinal cord and brain tissues exhibit motions, nevertheless these motions are limited to some situations like craniotomies and constrained in it is magnitude by the presence of the rigid skull and vertebras, which allows the application of IGNS with a proper compensation for these shifts. Preoperative tomograms and intra-operative dual fluoroscopy guided systems have been developed for spinal cord surgeries. [9]

Due to their precise localization of positions and angles, Image guided system have been used as well in orthopedics procedures successfully for artificial total hip and knee replacements, use in acetabulature fractures and in osteotomies were also realized In maxillofacial surgery they have been applied to insertion of dental implants. In abdominal, the situation is much different due to the unconstraint motion of the organs which make the realization of an accurate registration a very hard task. Moreover, the ongoing movements of organs like liver, heart and prostate due to both breathing and heart beats complicated the problem. Many attempted have been made to solve these problems in liver surgeries.

3.2.4 Adhesive skin marker

Adhesive skin marker are attached to the skin of the patient head prior to data acquisition and are defined as registration point at the start of the operation this is the most wide used registration method cutaneous marker systems are small plastic pads with adhesive on one side and a major diameter of 1-1.5 cm.they are fitted with radiopaque marker such as lead bead .at least four markers are placed on the patient until the start of the operation to allow the risk of premature marker loss.

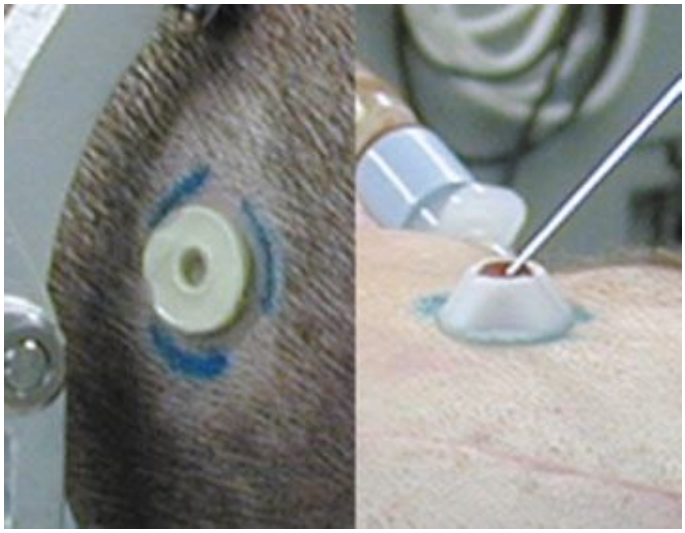

Figure 3.4 Adhesive skin markers [12]

3.2.5 Bone-mounted markers

Bone-mounted markers usually consist of 2 parts, a titanium base that is fixed into the patient skull and an exchangeable part that has filling depends on the used imaging modality. The filling could be made of a water solution containing x-ray contrast to be visible in both CT and MRI scans. Due to their rigid fixation, bone-mounted markers provided a solution to errors caused as a result of skin adhesive markers movement

It is often argued that the process of implanting such markers is an invasive procedure akin to the pin-mounting involved in fitting a stereotactic frame, Bone-mounted markers can provide the highest registration accuracy in the range of 0.5 to 1.5 mm, when they properly designed.[13]

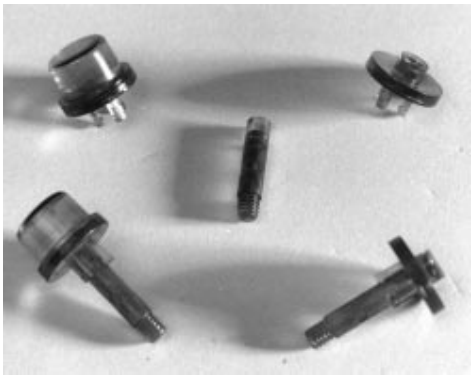

Figure 3.5 Bone-mounted markers [14]

3.2.6 Anatomical Landmark

ALS the development of increasingly powerful computers in the early 1990's led to the use of anatomical landmark for registration .the anatomical landmark are well defined structure usually bony prominence ,that provide definite reference points for instrument tracking . [14]

Registration with anatomical landmarks uses clearly defined external (such as nasion, spina nasalis, tragi, medial canthi, mastoid, umbo, and so on) and/or internal landmarks.

3.3 Registration Algorithms

Registration is the determination of a one-to-one mapping or transformation between the coordinates in one space and those in another, such that points in the two spaces that correspond to the same anatomical point are mapped to each other.[15]

From an operational view, the inputs of registration are the two views to be registered; the output is a geometrical transformation, which is merely a mathematical mapping from points in one view to points in the second.

There are many image registration methods, and they may be classified in many ways (Table 3.2) .our definition of registration is based on geometrical transformations, which are mappings of points from the space X of one view to the space Y of a second view.

3.3.1 Medical image registration classification

Table 3.2 Medical image registration classification criteria proposed by Maintz and Viergever (Maintz and Viergever, 1998)

<table>
<tr><th>Classification criteria</th><th colspan="3">Subdivision</th></tr>
<tr><td rowspan="2">Dimensionality</td><td colspan="3">Spatial dimension: 2D/2D, 2D/3D, 3D/3D</td></tr>
<tr><td colspan="3">Temporal series</td></tr>
<tr><td rowspan="11">Nature of the registration basis</td><td rowspan="4">Extrinsic (based on foreign objects introduced into the imaged space)</td><td rowspan="2">Invasive</td><td>Stereotactic frame</td></tr>
<tr><td>Fiducials (screw markers)</td></tr>
<tr><td rowspan="2">Non-invasive</td><td>Mould, frame, dental adapter, etc.</td></tr>
<tr><td>Fiducials (skin markers)</td></tr>
<tr><td rowspan="6">Intrinsic (based on patient)</td><td rowspan="2">Landmark based</td><td>Anatomical</td></tr>
<tr><td>Geometrical</td></tr>
<tr><td rowspan="2">Segmentation based</td><td>Rigid models (points, curves, surfaces, volumes)</td></tr>
<tr><td>Deformable models (snakes, nets)</td></tr>
<tr><td rowspan="2">Voxel property based</td><td>Reduction to scalars/vectors (moments, principal axes)</td></tr>
<tr><td>Using full image content</td></tr>
<tr><td colspan="3">Non-image based (calibrated coordinate systems)</td></tr>
<tr><td rowspan="4">Nature of transformation</td><td colspan="3">Rigid (only rotation and translations)</td></tr>
<tr><td colspan="3">Affine (translation, rotation, scaling and shearing)</td></tr>
<tr><td colspan="3">Projective</td></tr>
<tr><td colspan="3">Curved</td></tr>
<tr><td rowspan="2">Domain of transformation</td><td colspan="3">Local</td></tr>
<tr><td colspan="3">Global</td></tr>
<tr><td rowspan="5">Interaction</td><td rowspan="2">Interactive</td><td colspan="2">Initialization supplied</td></tr>
<tr><td colspan="2">No initialization supplied</td></tr>
<tr><td rowspan="3">Semi-automatic</td><td colspan="2">User initializing</td></tr>
<tr><td colspan="2">User steering/correcting</td></tr>
<tr><td colspan="2">Both</td></tr>
</table>

	Automatic
Optimization procedure	Parameters computed (the transformation parameters are computed directly)
	Parameters searched for (the transformation parameters are computed using optimization algorithms)
Modalities involved in the registration	Monomodal (CT/CT, MRI/MRI, PET/PET, CTA, etc.)
	Multimodal (CT/MRI, CT/PET, CT/SPECT, PET/MRI, MRI/US, etc.)
	Modality to model
	Patient to modality (align the patient with the coordinate system of the equipment)
Subject	Intrasubject (same subject)
	Intersubject (different subjects)
	Atlas
Object	Head (brain, eye, dental, etc)
	Thorax (entire, cardiac, breast, etc)
	Abdomen (general, kidney, liver, etc)
	Limbs
	Pelvis and perineum
	Spine and vertebrae

3.3.2 Registration algorithms

Registration algorithms implemented in image guided neurosurgery fields are mostly rigid, 3D, point-matching based techniques.

3.3.2.1 Affine transformations

A 3D affine transformation is given by

$$T(X) = D\,X + S \qquad (3.1)$$

Where *D* is a 3x3 matrix representing the rotation, scaling and shearing, and *S* is a 3x1 vector representing the translation or shift.

3.3.2.1.1 Rigid transformations

Is the simplest one, and in a 3D space, it can be defined by 6 parameters or degrees-of-freedom: 3 translational and 3 rotational parameters.

Surface registration method

Is to use the surface geometry of the face for image-to-patient registration, Using a surface-matching algorithm, a transformation is calculated that aligns both surfaces optimally. Computing the transformation by minimizing some measure of distance between the two surfaces.

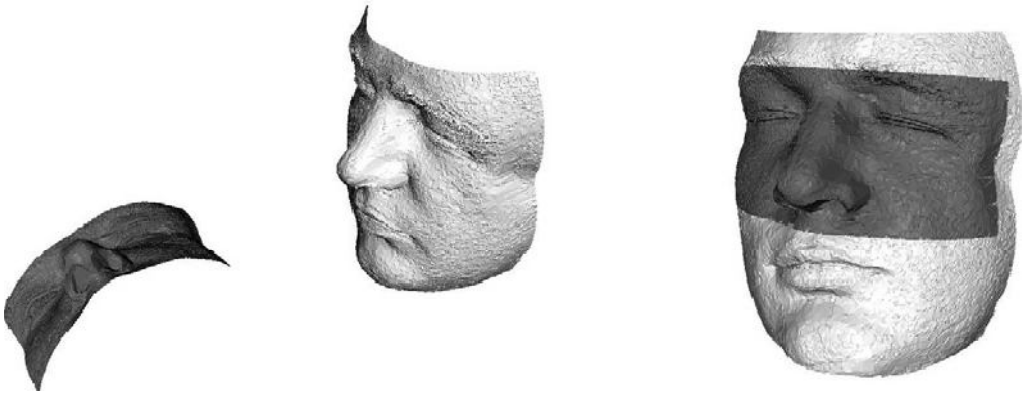

Figure 3.6 Concept of surface matching. Left: prior to registration, the two data sets that represent the same surface [16]

Point based registration

In pair-point registration, a set of at least three positions must be known in image space and physical space. These positions must be linearly independent (in this case, not lying on a line). By correlating these two sets of points in image data (by marking them on the computer screen) and physical space (by touching them with the tracked pointing device), both coordinate systems can be unambiguously registered. [16]

If some set of corresponding point pairs can be identified *a priori* for a given pair of views, then registration can be effected by selecting a transformation that aligns the points. Because such points are taken as being reliable for the purposes of registration, they are called *fiducial points*, or *fiducials*. To be reliable, they must lie in clearly discernible features, which we will call *fiducial features*. The determination of a precise point within a feature is called *fiducial localization*.

The fiducial localization process may be based on interactive visual identification of anatomical landmarks, such as the junction of two linear structures, e.g., the central sulcus with the midline of the brain or the intersection of a linear structure with a surface, e.g., the junction of septa in an air sinus, etc. alternatively, the feature may be a marker attached to the anatomy and designed to be accurately localizable by means of automatic algorithms.

3.3.2.1.2 Curved transformations

Their implementation is very simple as they can be defined by a deformation matrix and a translation vector. However, these transformations are rarely used since they do not usually represent the real deformations involved in the medical images.

3.3.2.1.3 Projective transformations

Preserve the straightness of lines and planarity of surfaces.

3.3.2.2 Intensity-based registration methods

Involves calculating a transformation between two images using the pixel or voxel values alone. In its purest form, the registration transformation is determined by iteratively optimizing some "similarity measure" calculated from all pixel or voxel values.

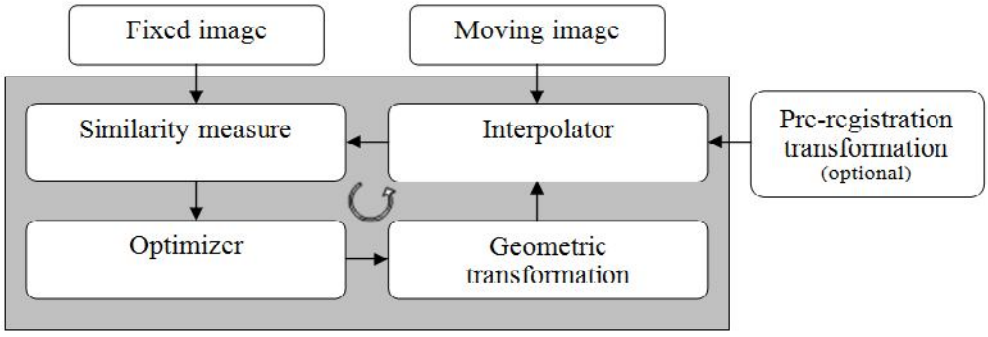

Figure 3.7 Diagram of the typical algorithms used in the intensity-based registration methodologies

3.3.2.3 Non Rigid transformations

The non-rigid transformation class includes the similarity transformation (translation, rotation and uniform scaling), affine (translation, rotation, scaling, and shear), projective, and curved. Non rigid transformations are important not only for applications to non rigid anatomy, but also for interpatient registration of rigid anatomy and intrapatient registration of rigid anatomy when there are non rigid distortions in the image acquisition procedure.

Scaling transformations

The simplest nonrigid transformations are rigid except for scaling,

$$X=R\ S\ X + T \qquad (3.2)$$

Where R is 3x3 orthogonal matrix ,S is a diagonal matrix whose elements represent scale factors along the three coordinate axes, T represent translation.

3.3.3 Comparison between points based registration algorithm and other available algorithms

1. In point-based registration there are a relatively small number of point pairs that describe corresponding locations in either coordinate system (image space and patient space) with high accuracy. In surface registration there are two large sets of points (hundreds, thousands or more) that describe the same surface, but there are no point pairs.
2. In intensity-based algorithms the amount of preprocessing or user-interaction required is much less than for point-based or surface-based methods.

3. The use of feature-based methods is recommended if the images contain enough distinctive and easily detectable objects. On the other hand point based registration performed whenever there are sets of point pairs
4. Intensity-based registration operates directly on the image grey values, while point based registration are not.

3.3.4 Evaluation of Registration Quality

Maurer et al. gave definitions of three errors in point-matching rigid registration: Fiducial Localization Error (FLE): the average error in locating the position of the fiducial points. Fiducial Registration Error (FRE): the Root Mean Square (RMS) distance between corresponding fiducial points after registration. Target Registration Error (TRE): the distance between corresponding points other than the fiducial points after registration.[17]

Recent studies have reported that it is not safe to use FRE only as estimation for the registration accuracy. It is only a rough evaluation of the actual accuracy (TRE) and is even found uncorrelated with it. TRE on the other hand, which is the most valuable estimation of the accuracy in IGNS, is not influenced only by FRE but also significantly by the number and the distribution of fiducial points.

CHAPTER FOUR

METHODOLOGY

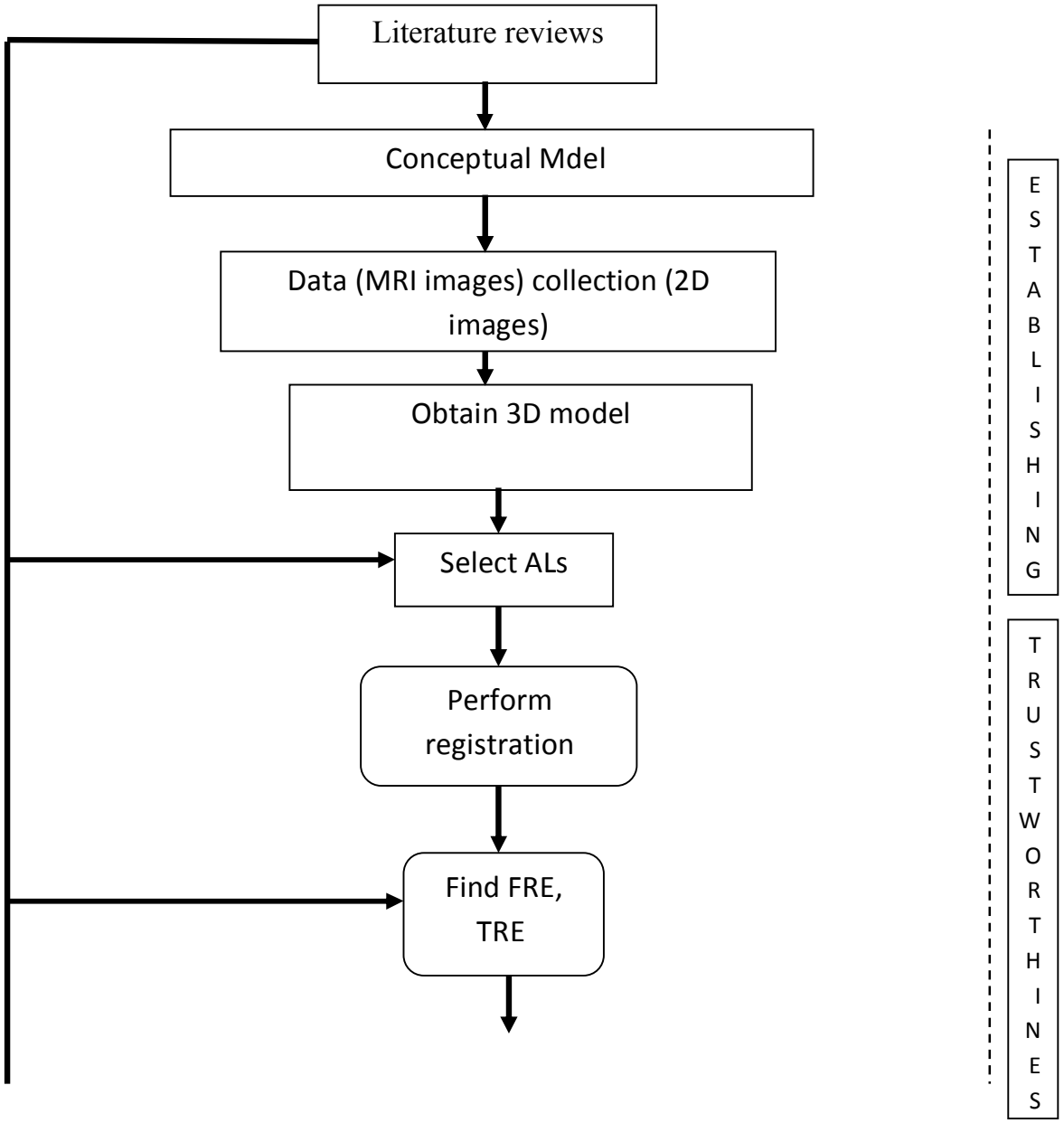

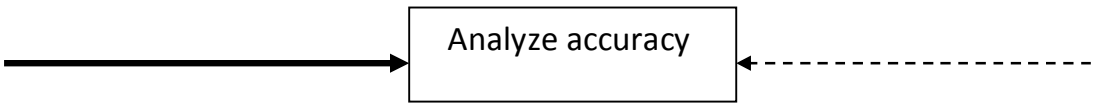

Figure 4.1 Design of the research

4.1 Establishing

It's begun By viewing of the literature review conceptual model formed and methodology started by collection of data which is two dimensional(2d) slices MRI images (224 slices),three dimensional (3d)image obtained from 2d slices using image reconstruction via MATLAB code(appendix).

Returning back to the literature review selected anatomical landmark (ALs) identified .then registration performed using point based registration algorithm via MATLAB code (appendix)

4.2 Trusting

It's begun by calculating of fidicual registration error (FRE) and target registration error (TRE) which were done via matlab code (appendix) after selection of fidicual points (ALs)and target points respectively.

Accuracy analysis and the comparison with calculated values in this project and those in the literature reviews explained in chapter five.

The whole system connected by **user interface system** (figure 4.2)

It's composed of one axis three push buttons the first push button (start) draw (2d) slices obtain 3 d. and the selection of ALs done within it. The second push button (find FRE calculate) FRE value and the third calculate the TRE values.

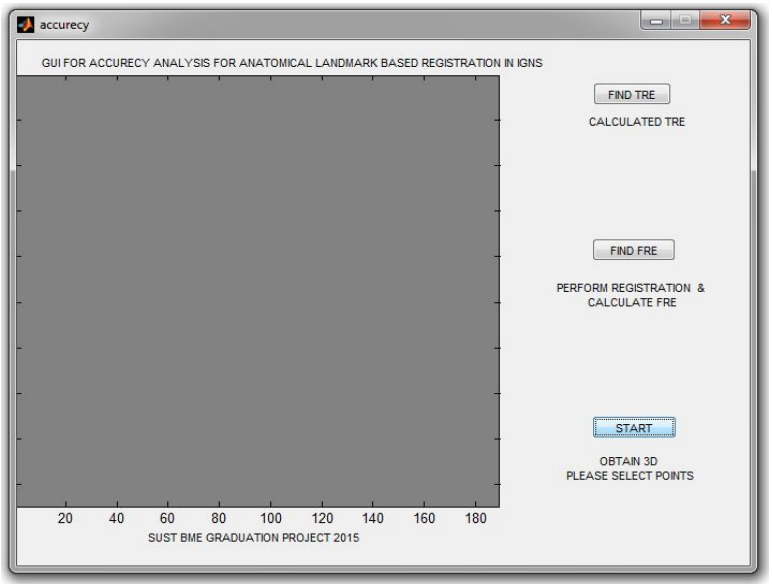

Figure 4.2 screen image of user interface system

CHAPTER FIVE

RESULTS AND CONCLUSIONS

Three kinds of results are proposed each of them clarify and analyze certain idea.

5.1 Subjectivity Analysis Result

It deals with the subjectivity and variation between the surgeons in the identification of the ALS, sample space consist of thirty random samples (table 5.1), selected from top senior medical student in ALAHFAD university.

The proposed ALS were glabella, tragus, lateral canthus and tip of the nose (figure 5.1)

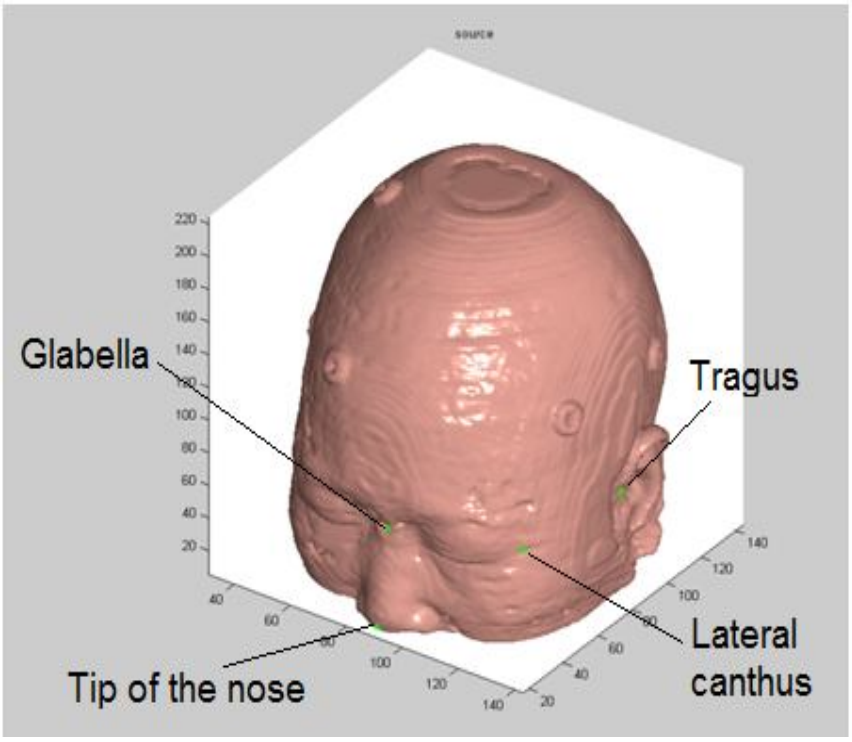

Figure 5.1 proposed ALs

Table 5.1 FRE and TRE for 30 random samples

No of samples	FRE	TRE
1	2.1822	2.6021 2.2159 3.0351 1.9233
2	3.3584	3.8841 3.9145 4.9073 2.8478
3	3.7106	4.9555 5.9311 6.9224 3.3131
4	2.4257	2.9322 3.0826 3.8723 2.0416
5	6.7796	8.2113 9.2634 11.1807 5.8429
6	3.5686	5.0847 5.7490 6.9643 3.3166
7	4.8404	6.3712 7.6403 8.8840 4.2994
8	1.3864	1.7984 1.8896 2.4368 1.1806
9	1.1632	1.5502 1.7737 2.1486 1.0165
10	2.0055	2.4750 2.8820 3.3341 1.7575
11	5.6552	7.3280 8.0474 10.0297 4.8150

12	2.6847	3.4057	3.4971	4.4974	2.3143
13	2.6847	3.4057	3.4971	4.4974	2.3143
14	1.0606	1.2421	1.4059	1.6328	0.9131
15	1.3454	1.5382	1.8045	2.0637	1.1256
16	1.5173	1.6453	1.7490	2.1078	1.2372
17	1.9935	2.3591	2.2948	2.9734	1.7012
18	1.7470	2.1556	2.6362	2.9661	1.5302
19	1.1415	1.3382	1.5057	1.7600	0.9787
20	1.4290	1.9225	2.1534	2.6244	1.2687
21	0.7609	0.8904	1.0072	1.1709	0.6551
22	3.0541	3.4640	4.0231	4.4984	2.6498
23	4.8243	6.0383	5.9486	7.8715	4.1214
24	2.212	2.4259	2.6789	3.1302	1.8483
25	2.4483	3.2084	3.5959	4.3503	2.1560
26	2.4774	3.1338	3.6226	4.3065	2.1239
27	0.8174	0.9519	1.0831	1.2489	0.7041
2 8	0.8991	1.0472	1.1911	1.3702	0.7763
29	1.0703	1.2482	1.4158	1.6355	0.9230
30	0.9657	1.1335	1.2868	1.4934	0.8311

5.1.1 Discussion

Mean and the standard deviation are calculated for FRE values the above result as a statistical analysis

$$\text{Mean} = \frac{\sum X}{N}$$

N≡ no of samples

X≡ value of each sample

$$\text{Mean}=\frac{71.4481}{30}=2.3816$$

Table 5.2 standard deviation calculation

N o of samples	FRE	FRE-mean	$(\text{FRE}-\text{mean})^2$
1	2.182	-0.1996	0.0398
2	3.3584	0.9768	0.9541
3	3.7106	1.329	1.7662
4	2.4257	0.0441	0.0019
5	6.7796	4.398	19.3424
6	3.5686	1.187	1.4089
7	4.8404	2.4588	6.0456
8	1.3864	-0.9952	0.9904
9	1.1632	-1.2184	1.4844
10	2.0055	-0.3761	0.1414
11	5.6552	3.2736	10.716
12	2.6847	0.3031	0.0918
13	2.6847	0.3031	0.0918
14	1.0606	-1.321	1.7450
15	1.3454	-1.0362	1.0737
16	1.5173	-0.8643	0.7470
17	1.9935	-0.3881	0.1506
18	1.7470	-0.6346	0.4027
19	1.1415	-1.2401	1.5378
20	1.4290	-0.9526	0.9074
21	0.7609	-1.6207	2.6266
22	3.0541	0.6725	0.4522
23	4.8243	2.4427	5.9667
24	2.212	-0.1696	0.0287
25	2.4483	0.0667	0.0044

26	2.4774	0.0958	0.0091
27	0.8174	-1.5642	2.4467
28	0.8991	-1.4825	2.1978
29	1.0703	-1.3113	1.7195
30	0.9657	-1.4159	2.0047
			$\sum(\text{FRE} - \text{mean})^2$ =67.0953

$$\sigma=\sqrt{\frac{\sum(\text{FRE}-\text{mean})^2}{n}}=\sqrt{\frac{67.0953}{30}}=\sqrt{2.23651}=1.4955$$

∴ Mean± σ =2.3816±1.4955

5.1.2 Summary

According to the values **3.2 mm±1.0** mm standard deviation using **NM 2.9±1.0** mm using **skin-adhesive** [3] **1.14** mm for **FM**, **2.3** mm for **AL**, and **0.96** mm for **SM** registrations [5] **calculated value in this project is in between**.

5.2 Repetitive Selection Analysis

It is used to analyze the accuracy of reselection of the same anatomical landmarks (ALS) by a surgeon; sample space consists of one sample which is a doctor in Khartoum hospital.

Table 5.3 Repetitive Selections FRE, TRE Values

No of irritation	FRE	TRE			
1	1.4446	6.3071	7.9895	9.5159	3.1697
2	0.8844	4.0977	5.2013	6.1914	2.0531
3	1.6702	7.6498	9.9330	11.7033	3.8210
4	1.8617	8.0546	10.5817	12.4591	3.9561

5.2.1 Discussion

We proposed calculating of the mean and the standard deviation for FRE values the above result as a statistical analysis

$$\text{Mean} = \frac{\sum X}{N}$$

N≡ no of samples

X≡ value of each sample

$$\text{Mean} = \frac{5.8609}{4} = 1.4652$$

Table 5.4 Standard Deviation Calculation for Repetitive Selection

N o of irritation	FRE	FRE-mean	$(\text{FRE} - \text{mean})^2$
1	1.4446	0.020625	0.0004
2	0.8844	0.5808	0.3373
3	1.6702	0.205	0.0420
4	1.8617	0.3965	0.1572
			$\sum(\text{FRE} - \text{mean})^2 = 0.5369$

$$\boldsymbol{\sigma} = \sqrt{\frac{\sum(\text{FRE}-\text{mean})^2}{N}} = \sqrt{\frac{0.5369}{4}} = \sqrt{0.134225} = 0.6053$$

5.2.2 Summary

According to the experiment Identification of the landmarks varied for one individual with a variation represented by the **standard deviation value** equal to **0.6053**

5.3 TRE values comparison

It is used to compare the variability on TRE values for each template compared to the others, frontal and parietal templates were used for this comparison.

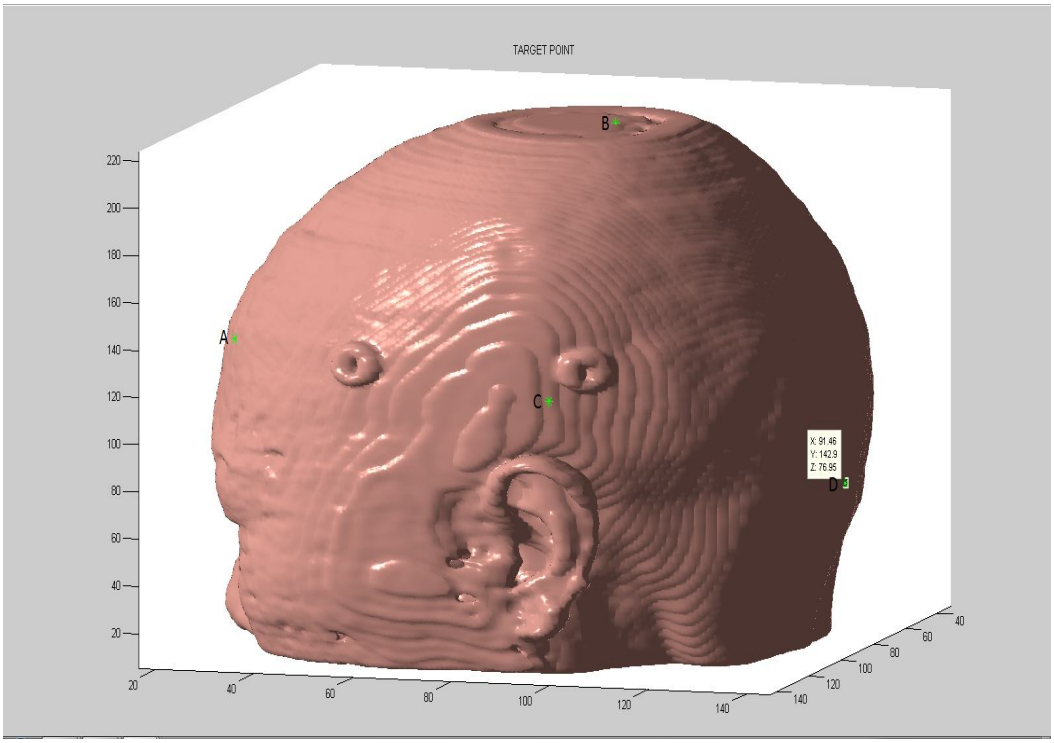

Figure 5.2 show target point (A point within frontal, B point within parietal, C point within temporal, D point within occipital)

Table 5.5 FRE, TRE Values for Templates

Template	**FRE**	**TRE**			
		A	B	C	D
Frontal	0.8357	1.6285	3.1282	1.4185	6.4482
Parietal	0.7351	4.6496	0.8390	4.4869	1.8165

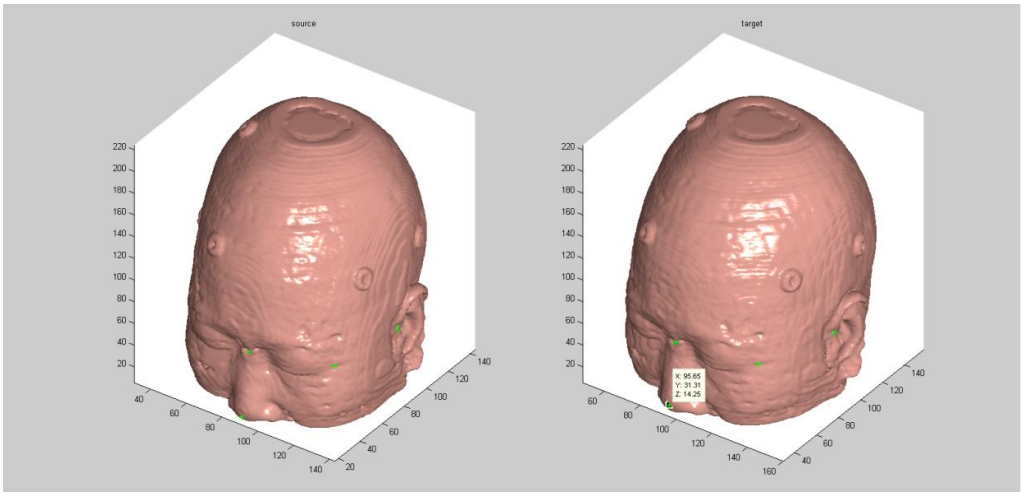

Figure 5.3 Frontal Template

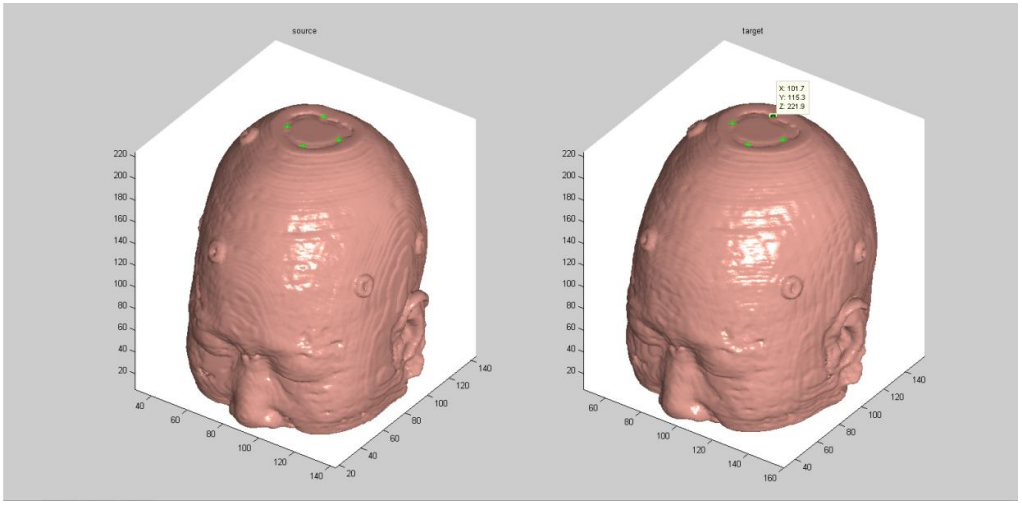

Figure 5.4 parietal template

Discussion

From the above table ; **point A** TRE varied from (**1.6285** to **4.6496**) so frontal template is better, **point B** TRE varied from(**3.1282** to **0.8390**) so parietal template is better, **point C** TRE varied from(**1.4185** to **4.4869**) so frontal template is better, **point D** varied from(**6.4482** to **1.8165**) so parietal template is better.

CHAPTER SIX

CONCLUSIONS AND RECOMMENDATIONS

6.1 Conclusions

1. Identification of the landmarks in both the patient and the image dataset is subjective.

2. Identification of the landmarks depends on the experience of the operator.

3. The variations on TRE values indicate that the closer target point to the point used to verify template the greater accuracy.

6.2 Recommendations

1. Generate the color code in order to visualize the difference in TRE from one region to another

2. Future work must include more target points in TRE calculation.

3. Try to connect the system with robotic surgery system in order to have an ideal result with ideal accuracy.

REFERENCE

[1] Current Problem in Surgery, Jcpsurg. September 2009.

[2] Computer Vision Method For Image Guided Surgery, Eric Grimson, Michael Leventon, Olivier Faugeras, William Wells, Cambridge MA,USA 02139.

[3].Anatomical Landmarks For Image Registration In Frameless Stereotactic Neuronavigation, Stefan Wolfsberger · K. Rössler · R. Regatschnig K. Ungersböck, 2002

[4] Image-Guided Surgical Planning Using Anatomical Landmark In The Retrosigmoid Approach, Erasmo Barros Da Silva Jr. & André G. Leal & Jerônimo B. Milano & Luis F. Moura Da Silva Jr. & Rogério S. Clemente & Ricardo Ramina, 2009.

[5] Fiducial Versus Nonfiducial Neuronavigation Registration Assessment and Considerations of Accuracy, Wolfgang K. Pfisterer, M.D., Wolfgang K. Pfisterer, M.D. and Denise A. Drumm, Ph.D 2008.

[6] Localisation of Anatomical Soft Tissue Landmarks of the Head in CT Images, M. Ovinis, D. Kerr, K. Bouazza-Marouf, and M. Vloeberghs 2010.

[7] Biofluid Dynamics In Human Head,Ranjith Pothagani , Rohit Kunadahaju 2013.

[8]Anatomy of Human Body Henry Gray 1918.

[9] Anatomical Landmarks For Point-Matching Registration In Image-Guided Neurosurgery,Akram I. Omara Manning Wang ,Yifeng Fan ,Zhijian Song March 2013.

[10] Needle Based Interventions With Image Guided Surgery Tool Kit (IGSTK) April 2010

[11] Image Guided Procedure April 2006

[12] Registration Accuracy And Practicability Of Laser-Directed Surface Matching, J. Schlaier, M.D., J. Warnat, M.D., And A. Brawanski, M.D., 2003

[13] Image-Guidance For Surgical Procedures, Terry M Peters, 2006

[14] Dryden, I.L., Mardia, K.V.: Statistical Shape Analysis. Wiley (1998)

[15] Registration Of Head Volume Images Using Implantable Fiducial Markers Calvin R. Maurer, Jr., *Member, Ieee*, J. Michael Fitzpatrick,* *Member, Ieee*, Matthew Y. Wang, *Student Member, Ieee*, Robert L. Galloway, Jr., *Member, Ieee*,Robert J. Maciunas, And George S. Allen, August 1997

[16] Image-To-Patient Registration Techniques In Head Surgery. G. Eggers, J. Mu¨Hling, R. Marmulla September 2006

[17] Improving Target Registration Accuracy In Image-Guided Neurosurgery By Optimizing The Distribution Of Fiducial Points Manning Wang Zhijian Song, *2008*

Appendix (A)

MATLAB code for accuracy analysis for anatomical land mark in image guided neurosurgery via user interface system

```
function varargout = accurecy(varargin)
% ACCURECY MATLAB code for accurecy.fig
%      ACCURECY, by itself, creates a new ACCURECY or raises the existing
%      singleton*.
%
%      H = ACCURECY returns the handle to a new ACCURECY or the handle to
%      the existing singleton*.
%
%      ACCURECY('CALLBACK',hObject,eventData,handles,...) calls the local
%      function named CALLBACK in ACCURECY.M with the given input arguments.
%
%      ACCURECY('Property','Value',...) creates a new ACCURECY or raises the
%      existing singleton*.  Starting from the left, property value pairs are
%      applied to the GUI before accurecy_OpeningFcn gets called.  An
%      unrecognized property name or invalid value makes property application
%      stop.  All inputs are passed to accurecy_OpeningFcn via varargin.
%
```

```
%      *See GUI Options on GUIDE's Tools menu.  Choose "GUI allows
only one
%      instance to run (singleton)".
%
% See also: GUIDE, GUIDATA, GUIHANDLES

% Edit the above text to modify the response to help accurecy

% Last Modified by GUIDE v2.5 11-Sep-2015 17:54:50

% Begin initialization code - DO NOT EDIT
gui_Singleton = 1;
gui_State = struct('gui_Name',       mfilename, ...
                   'gui_Singleton',  gui_Singleton, ...
                   'gui_OpeningFcn', @accurecy_OpeningFcn, ...
                   'gui_OutputFcn',  @accurecy_OutputFcn, ...
                   'gui_LayoutFcn',  [] , ...
                   'gui_Callback',   []);
if nargin && ischar(varargin{1})
    gui_State.gui_Callback = str2func(varargin{1});
end

if nargout
    [varargout{1:nargout}] = gui_mainfcn(gui_State, varargin{:});
else
    gui_mainfcn(gui_State, varargin{:});
end
% End initialization code - DO NOT EDIT
```

```
% --- Executes just before accurecy is made visible.
function accurecy_OpeningFcn(hObject, eventdata, handles, varargin)
% This function has no output args, see OutputFcn.
% hObject    handle to figure
% eventdata  reserved - to be defined in a future version of MATLAB
% handles    structure with handles and user data (see GUIDATA)
% varargin   command line arguments to accurecy (see VARARGIN)

% Choose default command line output for accurecy
handles.output = hObject;

% Update handles structure
guidata(hObject, handles);

% UIWAIT makes accurecy wait for user response (see UIRESUME)
% uiwait(handles.figure1);


% --- Outputs from this function are returned to the command line.
function varargout = accurecy_OutputFcn(hObject, eventdata, handles)
% varargout  cell array for returning output args (see VARARGOUT);
% hObject    handle to figure
% eventdata  reserved - to be defined in a future version of MATLAB
% handles    structure with handles and user data (see GUIDATA)

% Get default command line output from handles structure
```

```
varargout{1} = handles.output;



% --- Executes on button press in pushbutton1.
function pushbutton1_Callback(hObject, eventdata, handles)
% hObject    handle to pushbutton1 (see GCBO)
% eventdata  reserved - to be defined in a future version of MATLAB
% handles    structure with handles and user data (see GUIDATA)
filebase = 'C:\New DATA\';
startFrame = 1;
endFrame = 224;
%read frames, reduce size, show frames, and build volume
for r=startFrame:endFrame
    filename=[filebase,num2str(r,'%2d'),'.jpg'];
    temp=double(imresize(imread(filename), 0.5));
D(:,:,r) =temp;
    imagesc(D(:,:,r));
title('source')
    colormap('gray')
drawnow
end
%%%%%%%%%%%%%%%%%%%%%%%%%%%%%%%%%%%%%%%%%%%%%%%%%%%%%%%%%%%%%%%%%%%%%%%%%%%%%%%%%%%%%%%%%%%%%%%%%%%%%%%%%%%%%%%%%%%%%%%%%%%%%%%%%%%%%%
%
%file setup
filebase = 'C:\New DATA\';
startFrame = 1;
endFrame = 224;
```

```
%read frames, reduce size, show frames, and build volume
for r=startFrame:endFrame
    filename=[filebase,num2str(r,'%2d'),'.jpg'];
temp=double(imresize(imread(filename), 0.5));
temp = imrotate(temp,10,'bilinear');
D1(:,:,r) =temp;
    imagesc(D1(:,:,r));
title('target')
    colormap('gray')
drawnow
end
map=colormap;
figure('Colormap',map)
set(gcf, 'Position', get(0,'Screensize'));
ax1=subplot(1,2,1);
Ds = smooth3(D);
Fs = isosurface(Ds,7);
hiso = patch(isosurface(Ds,7),...
    'FaceColor',[1,.7,.65],...
    'EdgeColor','none');
hcap = patch(isocaps(D,7),...
    'FaceColor','interp',...
    'EdgeColor','none');
view(35,30)
% view(0,90)View the object from directly overhead.
axis tight
%daspect([1,1,.4])
```

```
lightangle(45,30);
set(gcf,'Renderer','zbuffer'); lighting phong
set(hcap,'AmbientStrength',.7)
set(hiso,'SpecularColorReflectance',0,'SpecularExponent',50)
title('source')
ax2=subplot(1,2,2);
Dt = smooth3(D1);
Ft = isosurface(Dt,7);
hiso = patch(isosurface(Dt,7),...
   'FaceColor',[1,.7,.65],...
   'EdgeColor','none');
hcap = patch(isocaps(D1,7),...
   'FaceColor','interp',...
   'EdgeColor','none');
view(35,30)
% view(0,90)View the object from directly overhead.
axis tight
%daspect([1,1,.4])
lightangle(45,30);
set(gcf,'Renderer','zbuffer'); lighting phong
set(hcap,'AmbientStrength',.6)
set(hiso,'SpecularColorReflectance',0,'SpecularExponent',50)
title('target')
%rotate and select control points
for i=1:4
h = rotate3d(ax1);
set(h,'RotateStyle','box','Enable','on');
pause
```

```
%continue
%hold
dcm_obj = datacursormode;
set(dcm_obj,'DisplayStyle','datatip',...
'SnapToDataVertex','off','Enable','on')
pause
%continue
%hold
info_struct = getCursorInfo(dcm_obj);
X(: , i) = info_struct.Position
hold all
plot3(X(1 , i), X(2 , i), X(3 , i), 'g*','markersize',9)
hold off
h = rotate3d(ax2);
set(h,'RotateStyle','box','Enable','on');
pause
%continue
%hold
dcm_obj = datacursormode;
set(dcm_obj,'DisplayStyle','datatip',...
'SnapToDataVertex','off','Enable','on')
pause
%continue
%hold
info_struct = getCursorInfo(dcm_obj);
Y(: , i) = info_struct.Position
hold all
plot3(Y(1 , i), Y(2 , i), Y(3 , i), 'g*','markersize',9)
```

```
hold off
end
save('bc.mat','X','Y')

% --- Executes on button press in pushbutton2.
function pushbutton2_Callback(hObject, eventdata, handles)
% hObject    handle to pushbutton2 (see GCBO)
% eventdata  reserved - to be defined in a future version of MATLAB
% handles    structure with handles and user data (see GUIDATA)
load  bc.mat
if nargin < 2
   error('At least two input arguments are required.');
end
[K N] = size(X);
[K_Y N_Y] = size(Y);
if K ~= K_Y
   error('X and Y must have the same number of rows.')
elseif (K ~= K_Y) || (N ~= N_Y)
   error('X and Y must have the same number of columns.');
end
if nargin >= 3
    w = ones(N,1);
   if ~isvector(w)
      error('w must be a vector');
   end
   if length(w) ~= N
      error('length of w must equal number of columns in X and Y');
   end
```

```
  w = w(:); % force it to be a column vector
end
if nargin < 4
  n_t = N; % User wants to use all points to compute translation
elseif n_t > N
  n_t = N; % because larger numbers make no sense
elseif n_t < 0
  n_t = 0;  % because negative numbers make no sense
end

% Calculate normalized weights and centroids:
w_sqr = w.^2;
sum_w_sqr = sum(w_sqr);
w_sqr_normed = w_sqr/sum_w_sqr;
if n_t == 0
  Xbar = zeros(K,1); Ybar = zeros(K,1); % dummy centroids
else
  w_sqr_n_t = w_sqr(1:n_t);
  w_sqr_n_t_normed = w_sqr_n_t/sum(w_sqr_n_t); % normed over first
n_t weights
  Xbar = X(:,1:n_t)*w_sqr_n_t_normed;  % X weighted centroid of first
n_t points
  Ybar = Y(:,1:n_t)*w_sqr_n_t_normed;  % Y weighted centroid of first
n_t points
end

% Demean the first n_t points:
Xtilde = X - [repmat(Xbar,1,n_t),zeros(K,N-n_t)];
```

```
Ytilde = Y - [repmat(Ybar,1,n_t),zeros(K,N-n_t)];

% Calculate the rotation:
H = Xtilde*diag(w_sqr_normed)*Ytilde';  % cross covariance matrix
[U S V] = svd(H);      % U*S*V' = H (change S to ~ for later Matlab versions)
D = diag([ones(1,K-1), det(V*U)]); % used to insure that R is proper
R = V*D*U';

% Calculate the translation:
t = Ybar-R*Xbar;

% Finish generating output:

  if n_t ~= N
    T = [repmat(t,1,n_t),zeros(K,N-n_t)];
  else
    T = repmat(t,1,N);
  end
  FREcomponents = repmat(w',K,1).*(R*X + T - Y);
  FRE = sqrt(FREcomponents(:)'*FREcomponents(:)/sum_w_sqr)
save('bc.mat','FRE','X','Y')

% --- Executes on button press in pushbutton3.
function pushbutton3_Callback(hObject, eventdata, handles)
% hObject    handle to pushbutton3 (see GCBO)
% eventdata  reserved - to be defined in a future version of MATLAB
% handles    structure with handles and user data (see GUIDATA)
```

```
load  bc.mat
[K,N] = size(Y);
meanY = mean(Y')';
Yc = Y-meanY*ones(1,N);  % demeaned Y
[V, Lambda, U] = svd(Yc);
T=[  111.0000   86.9999   137.7527   91.4573;25.6543   94.9193   97.9871
142.8632;135.0000 223.8657 123.1839 76.9466];
[K,M_T] = size(T);
Tc = T- meanY*ones(1,M_T);  % T relative to centroid of Y
Tv = V'*Tc;
% T referred to principal axes of Y
% Distances of target to the markers' three principal axes:
DI1 = Tv(2,:).^2 + Tv(3,:).^2;
DI2 = Tv(3,:).^2 + Tv(1,:).^2;
DI3 = Tv(1,:).^2 + Tv(2,:).^2;
% RMS distances of markers to their three principal axes:
F1 = (Lambda(2,2)^2 + Lambda(3,3)^2)/N;
F2 = (Lambda(3,3)^2 + Lambda(1,1)^2)/N;
F3 = (Lambda(1,1)^2 + Lambda(2,2)^2)/N;
TRE= sqrt((FRE^2/(N-2))*(1 + (1/3)*(DI1./F1 + DI2./F2 + DI3./F3)))
```